Applied Geochemistry 83 (2017) 136–149

Contents lists available at ScienceDirect

Applied Geochemistry

journal homepage: www.elsevier.com/locate/apgeochem

Stream hydrology and geochemistry along a rural to urban land use gradient

Elizabeth A. Hasenmueller [a,*], Robert E. Criss [b], William E. Winston [c], Andrew R. Shaughnessy [a]

[a] Department of Earth and Atmospheric Sciences, Saint Louis University, Saint Louis, MO, USA
[b] Department of Earth and Planetary Sciences, Washington University, Saint Louis, MO, USA
[c] Data and GIS Services, Washington University, Saint Louis, MO, USA

ARTICLE INFO

Article history:
Received 1 July 2016
Received in revised form 11 December 2016
Accepted 16 December 2016
Available online 18 December 2016

Keywords:
Urban streams
Stream chemistry
Land use/land cover
Flooding
Isotope hydrology
Hydrograph separations

ABSTRACT

High frequency monitoring of water quality and stable isotopes quantify large hydrological and geochemical differences across a rural to urban land use gradient that includes three watersheds and two of their subbasins. Following precipitation events, floods on a rural stream feature hydrographs with low peak discharges and long lag times, high baseflow contributions, and small geochemical variations. In contrast, the flows of an urban stream and its tributary respond in a flashy manner, with average lag times decreasing by at least 55% compared to the rural stream. We also observed that baseflow contributions during floods decreased by an average of 40% in the urban streams. Importantly, we find that reduced baseflow as a function of increasing impervious surface area is not a linear trend among the streams, and suburban streams are less impacted than would be predicted by impervious surface area alone. The urban streams also exhibit large variations in water quality parameters during flooding events, often with five times the variability of the rural end-member. These differences are observed among all physical and geochemical characteristics that were monitored, including flow magnitude, stable isotope ratios, temperature, dissolved oxygen (DO), pH, turbidity, specific conductivity, concentrations of Cl^- and nutrients, and bacterial loads. The great variability of urban streams following storms is paralleled by their larger diurnal and seasonal oscillations. Collectively, the extreme variations in the physical and geochemical character of urban streams have negative consequences to environmental quality and aquatic life.

1. Introduction

Streams in urban areas feature frequent flash flooding and have numerous point and non-point sources that degrade water quality. Transient storm events exacerbate these problems because large volumes of runoff are rapidly delivered to streams due to increased impervious surface area (O'Driscoll et al., 2010; Kaushal et al., 2015), thus transporting water, sediments, and pollutants at rates that can dwarf their delivery during normal flows (Ogden et al., 2000; Borah et al., 2003; Konrad, 2003; Vicars-Groening and Williams, 2007; Hasenmueller and Robinson, 2016). Understanding the processes that generate flow in urban streams during flood events is critical to managing the effect on water quantity and quality. Indeed, urban land use can considerably modify the flooding response of streams, leading to higher peak discharges, shorter and sharper rising and recessional limbs of the hydrograph, and higher runoff volumes relative to their undisturbed, rural counterparts (Arnold and Gibbons, 1996; Walsh et al., 2005; Burns et al., 2012). One of the main drivers of altered hydrologic response for urban streams is high impervious surface area (Endreny, 2005; Burns et al., 2012). Many studies have tried to model the extent to which impervious surface area enhances event water inputs from recent rainfall events (Brabec et al., 2002; Jennings and Jarnagin, 2002). Yet, using total impervious surface area in a watershed can lead to overestimates of event water volume and peak discharge as well as pollutant loads associated with the event water component (Alley and Veenhuis, 1983; Brabec et al., 2002; Lee and Heaney, 2003; Loperfido et al., 2014).

Two-component isotopic hydrograph separations are a valuable tool in understanding the relative contributions of "new" event water (i.e., recent rainfall) and "old" pre-event baseflow (i.e., groundwater). However, few such studies have been conducted in suburban and urban environments; instead, most have been

* Corresponding author.
E-mail address: hasenmuellerea@slu.edu (E.A. Hasenmueller).

http://dx.doi.org/10.1016/j.apgeochem.2016.12.010
0883-2927/

performed in humid, temperate, forested catchments (Sklash and Farvolden, 1979; Sklash et al., 1986; Buttle and Sami, 1992; Renshaw et al., 2003; Klaus and McDonnell, 2013). Results from rural areas generally show that streamflow during flooding is largely supplied by older groundwater and soil water reservoirs stored in the catchment prior to the rainfall or snowmelt event, usually comprising 70 ± 20% of peak streamflow (Sklash and Farvolden, 1979; Sklash et al., 1986; Buttle and Sami, 1992; Genereux and Hooper, 1998; Brown et al., 1999; Renshaw et al., 2003; Winston and Criss, 2004; Stueber and Criss, 2005; Muñoz-Villers and McDonnell, 2012).

Surprisingly few studies attempt to resolve the relative contributions of different runoff fractions in catchments that feature other land uses, including suburban and urban land use. Buttle et al. (1995) conducted early studies of runoff components in small, suburban systems during snowmelt and found high contributions of event water during stormflow, specifically comprising 48–58% of the total runoff and >55% of peak flow. More recent studies have encompassed land use and land cover changes in larger and more diverse basins. Gremillion et al. (2000) studied a Florida river and found that stormflow increased by 29% along a reach with higher suburban land use than an upstream, forested reach, indicating changes to water flowpaths from urbanization. A high (and highly pulsed) event water component was also observed in a small, urban watershed in Massachusetts, where event water comprised 18–78% (average = 51%) of the total flow and 5–97% (average = 60%) of peak flow (Pellerin et al., 2008) during 19 studied flood events. A study in central Pennsylvania, which included forested, agricultural, urban, and two mixed land use catchments, showed that event water dominated peak flow in the urban catchment (average = 69%), but represented <25% of peak flow in the forested and agricultural catchments (Buda and DeWalle, 2009). Meriano et al. (2011) dispute the commonly held view that pre-event water contributions stored in urban basins are too small to influence streamflow rates significantly. Their study of a highly urbanized (87% urban land use), 7.6 km^2 watershed in southcentral Ontario found that groundwater contributed 22% of the total stormflow. Indeed, Jefferson et al. (2015) found that stormwater control measures, used to mitigate problems with runoff in an urban North Carolina catchment, contributed an average of 10% of streamflow on the rising limb of flood hydrographs, but up to 32% on the falling limb.

Importantly, of the handful of studies that quantified streamflow components in suburban and urban streams, most focus on a single catchment and/or only consider the flooding response to a single precipitation event. To our knowledge, no studies have systematically assessed flood response along a rural to urban gradient, nor examined watersheds with exclusively urban land cover (i.e., 100%), both of which are crucial to understand rainfall-runoff patterns and pollutant transport in developed watersheds. Here, we deliberately examined three watersheds and two of their subbasins along a gradient of increasing impervious surface area in highly urbanized Saint Louis, Missouri, to quantify changes in the relative contributions of pre-event water and event water to streamflow during flooding. In addition to quantifying the differences in hydrologic response among our watersheds, we also compare individual chemical constituents in streamflow to determine short-term (i.e., flooding and diurnal) and long-term (i.e., seasonal) geochemical variability as a function of land use.

2. Materials and methods

2.1. Site descriptions

We concurrently monitored the hydrology and geochemistry of five watersheds featuring differing land use in the Saint Louis, Missouri, metropolitan area between October 2007 and September 2008. The watersheds fall along a southwest to northeast transect that was carefully selected to represent a gradient in urban land use, from a forest-dominated watershed west of the city to highly urbanized watersheds in the city center (Fig. 1). Our study area features similar regional climate, lithology, and vegetation to minimize the effects of other basin properties besides land use on the hydrology and geochemistry. The southwest to northeast orientation of the transect reduced meteorological differences between the basins because it follows the predominant storm path in this region, so the study basins are generally aligned to intersect the same storms. Regional geology generally consists of Paleozoic carbonates. Monitoring sites were located near the mouth of each catchment (Fig. 1) proximal to U.S. Geological Survey (USGS) discharge gauging stations (Table 1).

2.1.1. Rural stream: Fox Creek

Fox Creek (46.3 km^2), located in the Meramec River basin, has an average discharge of 0.51 m^3/s. It serves as the rural end-member in our interbasin comparison, with only 1.5% impervious surface area and 9.4% developed area (Table 1; Multi-Resolution Land Characteristics Consortium; MRLC, 2016). Properties in the watershed are large and dispersed and include a few small farms (Fig. 1). While the watershed is still largely rural, it is beginning to experience residential and commercial growth, and a major highway (I-44) crosses this basin near its confluence with the Meramec River. Fox Creek has relatively good water quality and hosted 44 species of fish in 2005 (Missouri Department of Conservation; MDC, 2005), but was more recently listed as impaired in aquatic macroinvertebrate bioassessments on the U.S. Environmental Protection Agency's (USEPA) 2012 Missouri 303d list (Missouri Department of Natural Resources; MoDNR, 2016). The geology predominantly consists of Ordovician limestone and dolostone units. Basin elevations range from 245 m at the headwaters to 133 m at the confluence with the Meramec River.

2.1.2. Suburban streams: Grand Glaize Creek and Sugar Creek

Grand Glaize Creek (61.4 km^2) is a suburban stream also located in the Meramec River watershed and has an average discharge of 0.68 m^3/s. The Grand Glaize Creek basin is located near Valley Park, Missouri (Fig. 1), and exhibits extensive residential development, with 26.1% impervious surface area and 77.5% developed area (Table 1; MRLC, 2016). The catchment is situated near the interstate highway bypass (I-270) that surrounds the greater metropolitan Saint Louis area. It exhibits several water quality issues including high Hg levels in fish tissues, high Cl^-, bacterial contamination, and low DO (see the 2002–2014 USEPA-approved 303d lists for Missouri; MoDNR, 2016). Wildlife has been heavily impacted by development in the basin, and in 2005, the stream only hosted 7 species of fish (MDC, 2005). The catchment is underlain predominantly by Mississippian limestones, but basin geology also includes Pennsylvanian shales in the eastern portion of the watershed. Basin elevations range from 200 m at the head waters to 120 m at the stream outlet. Sugar Creek is a small (13.3 km^2) tributary to Grand Glaize Creek with 25.9% impervious surface area and 81.6% developed area (Table 1). The stream has an average discharge of 0.17 m^3/s. In 2005, the stream hosted 6 species of fish (MDC, 2005). Upland areas include Pennsylvanian shales, while Mississippian limestones dominate the lowland areas.

2.1.3. Urban streams: River des Peres and Black Creek

The River des Peres is a large (295.0 km^2), highly degraded watershed draining densely urbanized areas in Saint Louis and represents the urbanized end-member for this comparative study

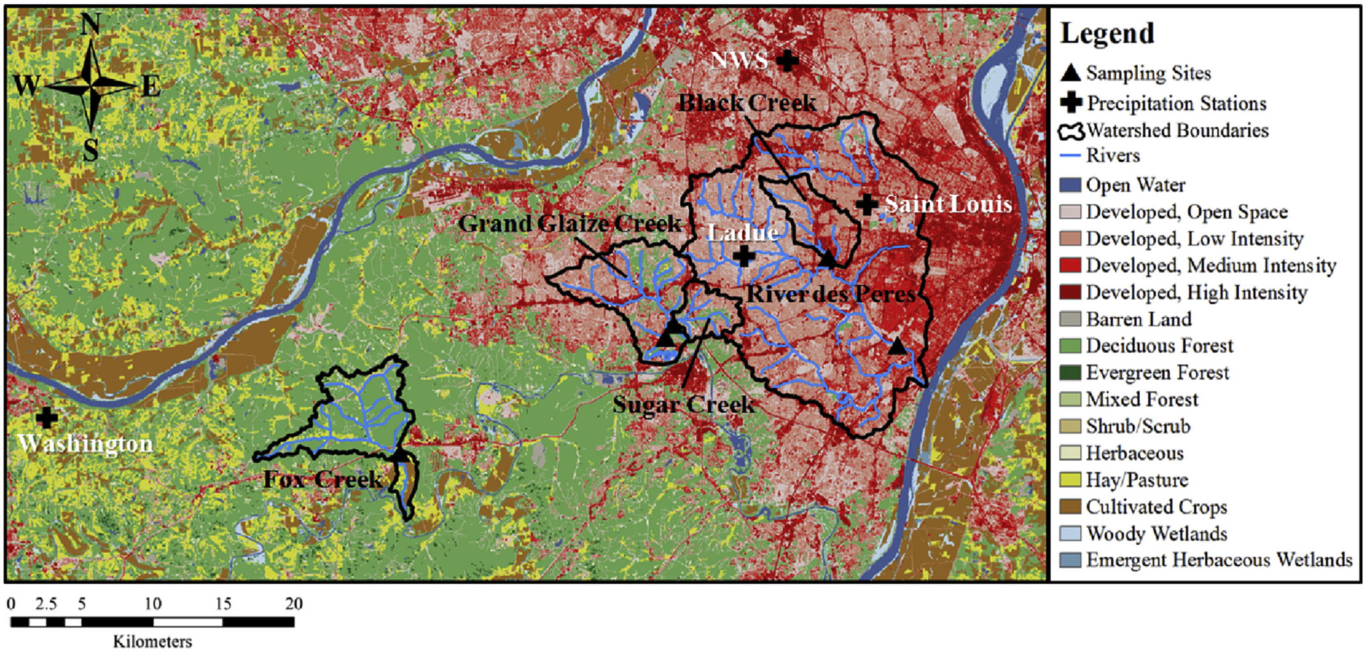

Fig. 1. Map of the stream sampling sites and precipitation monitoring locations. Watershed boundaries are delineated on a land use/land cover map of east-central Missouri (2006 National Land Cover Database; MRLC, 2016) and each watershed is labeled with black text. The NWS (NOAA, 2016), Saint Louis, Ladue, and Washington precipitation stations are labeled with white text. Detailed surface water hydrology is shown for the watersheds of interest; note that portions of the River des Peres and its tributaries are piped underground in some of the most densely urbanized portions of Saint Louis.

Table 1
Stream sampling site information, watershed land use/land cover from MRLC (2016), and hydrologic response parameters.

Parameter	Fox Creek	Grand Glaize Creek	Sugar Creek	River des Peres	Black Creek
Watershed Area (km^2)	46.3	61.4	13.3	295.0	22.4
Stream Order	4	4	3	5	3
Hydrologic Unit[a]	07140102	07140102	07140102	07140101	07140101
USGS Gauging Station Number	07017115	07019185	07019175	07010097	07010082
Impervious Surface Area (%)	1.5	26.1	25.9	39.5	41.2
Open Water (%)	0.1	0.8	None	>0.1	None
Developed, Open Space (%)	6.8	20.0	20.8	19.5	15.2
Developed, Low Intensity (%)	2.2	44.1	49.8	51.5	57.8
Developed, Medium Intensity (%)	0.4	9.2	7.5	19.3	15.5
Developed, High Intensity (%)	>0.1	4.2	3.5	8.7	11.5
Barren Land (%)	None	>0.1	None	>0.1	None
Deciduous Forest (%)	69.1	19.5	17.4	0.7	None
Evergreen Forest (%)	0.8	>0.1	None	>0.1	None
Mixed Forest (%)	0.3	0.2	0.1	>0.1	None
Shrub/Scrub (%)	>0.1	>0.1	None	None	None
Herbaceous (%)	1.9	0.1	0.2	>0.1	None
Hay/Pasture (%)	12.5	0.4	0.1	None	None
Cultivated Crops (%)	5.4	0.1	0.1	None	None
Woody Wetlands (%)	0.3	1.3	0.5	0.1	None
Emergent Herbaceous Wetlands (%)	None	None	None	>0.1	None
Ave. Lag Time (h)	4.8	3.8	2.4	2.1	1.3
Ave. Baseflow: SpC Separations (%)	61	51	NA	72[b]	24
Ave. Baseflow: $\delta^{18}O$ Separations (%)	62	55	NA	NA	22

[a] See USGS (2016) for hydrologic unit explanation.
[b] Average baseflow percentage determined by specific conductivity (SpC) hydrograph separations for the River des Peres only includes flood events from October to mid-December 2007 when the stream was not affected by road salting or Mississippi River backwater. See Fig. 2B for comparisons with Fox Creek and Grand Glaize Creek during the same time interval.

(Fig. 1). The watershed features 39.5% impervious surface area and 99.0% developed land (Table 1; MRLC, 2016). The river extends approximately 30 km through Saint Louis before discharging into the Mississippi River. Most of the mainstem (>80%) was straightened and channelized using a system of tunnels, pipelines, and canals during the River des Peres Sewerage and Drainage Works project (1924–1931) in an attempt to mitigate flooding issues and alleviate severe water quality problems associated with both accidental and intentional use of the river as an open sewer (Corbett, 1997; Shock et al., 2003; ASCE, 2016). Flow rates on the River des Peres are highly variable (Hasenmueller and Robinson, 2016) and can range from nearly zero to more than 700 m^3/s during floods (average = 2.17 m^3/s; USGS, 2016). The watershed hosts 134 combined sewer overflows (CSOs) along its reaches, and about 50 overflows per year discharge 24,000,000 m^3 annually (Metropolitan Saint Louis Sewer District; MSD, 2016). The River des Peres mainstem has high Cl^-, bacterial contamination, and low DO (see the 2002–2014 USEPA-approved 303d lists for Missouri; MoDNR, 2016). The geology of the basin consists predominantly of the Mississippian limestones in the southwest and Pennsylvanian shales in the northeast. These units are overlain by Quaternary loess soils (Lutzen and Rockaway, 1989; Harrison, 1997). Elevations in the basin range from 200 m in the headwaters to 140 m at the River des Peres' confluence with the Mississippi River.

Black Creek is a small tributary (22.4 km^2) to the River des Peres, which drains commercial areas in the Saint Louis suburb of Brentwood, Missouri (Fig. 1). The area is fully (i.e., 100%) developed, with 41.2% impervious surface area (Table 1; MRLC, 2016). Additionally, much of this stream is confined in cement-walled channels or culverts. Discharge ranges from virtually zero to almost 150 m^3/s during floods, with an average of 0.22 m^3/s (USGS, 2016). The stream also features many CSOs as well as several detention basins used for flood control. The catchment exhibits poor water quality including high Cl^- and bacterial contamination (i.e., 2002–2014 USEPA-approved 303d lists for Missouri; MoDNR, 2016). The geology of the basin consists mostly of Pennsylvanian shales, but includes small areas of Mississippian limestones in lowland areas. These units are overlain by Quaternary loess soils (Lutzen and Rockaway, 1989; Harrison, 1997).

2.2. Field methods

To understand the effect of land use on short-term (i.e., flood and diurnal response) and long-term (i.e., seasonal) watershed hydrology and geochemistry, the catchments along the land use gradient were monitored for a one year period (October 2007 to September 2008). Monitoring efforts included field grab sampling, high frequency sampling during floods, and continuous in situ monitoring of water quality parameters. Sites were visited on a biweekly basis to collect samples for lab analyses and measure temperature, dissolved oxygen (DO), pH, turbidity, and specific conductivity with handheld meters. The Cl^-, NH_4^+-N, NO_3^--N, and total P as PO_4^{3-} levels in unfiltered stream samples were collected in pre-cleaned high density polyethylene (HDPE; Cl^-, NH_4^+-N, NO_3^--N) or glass (total P) bottles. Subsamples for N-species and total P were field-acidified with concentrated H_2SO_4 to pH < 2. *Escherichia coli* (*E. coli*) subsamples were collected in pre-cleaned, autoclaved HDPE bottles. All samples for ions and bacterial analyses were stored on ice until returning to the lab. Field duplicates were collected approximately every other visit. Automated sampling devices (ISCO models 3700 or 6712) collected high frequency water samples from Fox Creek, Grand Glaize Creek, and Black Creek during flooding events; typically, 10–60 samples per precipitation event were collected with the autosamplers to characterize floods. It was not feasible to deploy autosamplers at the Sugar Creek or River des Peres sites.

In situ monitoring devices were installed at four sites to continuously measure water quality parameters and record data at 5-min intervals. At Fox Creek, Grand Glaize Creek, and the River des Peres, YSI 6600V2 sondes measured temperature, DO, pH, turbidity, specific conductivity, Cl^-, and NH_4^+-N. During a portion of our study (June to July 2008), the autosampler at Black Creek was equipped with a YSI 600 sonde that continuously measured temperature, DO, pH, and specific conductivity, but only when the autosampler was activated during flood events. All sondes were calibrated during biweekly sampling visits. Nearby USGS gauging stations provided all stream discharge data used in this study (USGS, 2016).

Precipitation samples were collected from three rain gauges in Saint Louis, Ladue, and Washington, Missouri, to characterize rainfall amounts and chemical variability across the land use gradient (Fig. 1). We collected total precipitation for each event of interest and time series samples every 4–6 h for some storms. The specific conductivity of a subset of precipitation samples (n = 10) was measured immediately after collection from the Saint Louis rain gauge; these measurements were averaged and used for specific conductivity hydrograph separations (see section 2.4). Subsamples for isotopic analyses were also collected. In addition to rain gauge samples, hourly precipitation totals measured by the National Weather Service (NWS) at Lambert-Saint Louis International Airport (National Oceanic and Atmospheric Administration; NOAA, 2016; Fig. 1) were used for higher temporal resolution during precipitation events.

2.3. Lab methods

Field samples were separated for geochemical analyses. Untreated precipitation and stream samples were analyzed for H and O isotope compositions using an isotope ratio mass spectrometer (IR-MS; Thermo Finnigan MAT 252). We used standard analytical methods (Hasenmueller and Criss, 2013) and report δD and $\delta^{18}O$ values relative to V-SMOW; precision is ±1.0‰ and ±0.1‰, respectively. In the following, we always report δD and $\delta^{18}O$ values in that order. All subsamples for ions were refrigerated after field collection until analysis. We determined Cl^-, NH_4^+-N, NO_3^--N, and total P concentrations with colorimetry using USEPA-approved techniques (Hach, 2005a–e). The IDEXX Colilert reagent and 97-well Quanti-Tray® were used to count *E. coli* colonies; the method is USEPA-approved and has a most probable number range of 1–2420 cfu/100 mL. All labware for bacterial analyses was autoclaved before use. Lab duplicates, triplicates, and matrix spikes, along with field duplicates, were run to determine method accuracy. Lab duplicates and triplicates were analyzed approximately every 10 samples for each lab method. Matrix spikes were also analyzed approximately every 10 samples, but only for Cl^-, NH_4^+-N, NO_3^--N, and total P. Field duplicates and lab duplicates, triplicates, and matrix spikes varied by no more than ±20% for ions.

2.4. Hydrograph separations

Isotope and specific conductivity data collected during flood events were used in two-component hydrograph separations (Sklash and Farvolden, 1979) to calculate the absolute and relative contributions of "old" water (baseflow) and "new" water (event water) to the streams. This relationship of pre-event water and event water can be described with the following equations:

$$Q_t = Q_b + Q_e \quad (1)$$

$$Q_tC_t = Q_bC_b + Q_eC_e \quad (2)$$

$$X_b = \frac{C_t - C_e}{C_b - C_e} \quad (3)$$

where Q is the discharge, C is the tracer value (isotope or specific conductivity value), the subscripts represent the total (t), baseflow (b), or event water (e) discharge or tracer value, and X_b is the baseflow fraction, which is equal to Q_b/Q_t. In this study, baseflow was defined as the tracer value in the stream 48 h prior to the precipitation event (Buttle et al., 1995; Heppell and Chapman, 2006; Pellerin et al., 2008). Baseflow was characterized by low discharge values, isotope values close to the weighted, long-term average of local meteoric precipitation (i.e., −45‰ and −7.0‰; see Criss, 1999), and specific conductivity values near the seasonal average for the stream. Event water was defined by the isotope values of time series or aggregate precipitation samples or the averaged specific conductivity of a subset of precipitation samples (average = 54 μS/cm, standard deviation = 6 μS/cm, $n = 10$). Event water exhibits higher discharge values, variable isotope compositions, and relatively low specific conductivity compared to baseflow.

The two-component hydrograph method requires some simplifying assumptions to be valid. For this study, we assumed that tracer values: (1) in soil water and groundwater are similar, (2) remain relatively uniform along flowpaths to the stream of interest, and (3) are representative of baseflow in stream water 48 h prior to the flood event of interest, except when storms occurred in rapid succession, in which case we used tracer values 48 h before the first flood event. During low flow periods prior to storm events, specific conductivity did not vary more than ±10%, but to fulfill our second assumption, we did not use specific conductivity for hydrograph separations when deicing chemicals were applied to the roads during winter months (i.e., mid-December 2007 to mid-March 2008) as road salt application would change the chemical character of event water along the flowpath. Isotope hydrograph separations presented below are all derived from $\delta^{18}O$ values since there was good agreement (within 5%) for the same flood events using H or O isotopes.

3. Results

3.1. Flood response across a rural to urban gradient

3.1.1. Hydrograph separations

We examined the flooding behavior of Fox Creek, Grand Glaize Creek, the River des Peres, and Black Creek to determine the effect of land use on their physical response to rainfall events. We analyzed variations among the sites in the: (1) overall shape and timing of the hydrograph, including peak flows and lag times (i.e., the time interval from the center of mass of rainfall to peak discharge), (2) relative contributions and timing of baseflow and event water, and (3) flow responses to differing rainfall amounts and antecedent moisture conditions.

The flood hydrograph of our rural end-member, Fox Creek, was less responsive to precipitation events, with rainfall amounts as large as 0.8 cm and with intensities of nearly 0.4 cm/h often resulting in no discharge response. In contrast, rainfall events as small as 0.05 cm and with intensities of 0.02 cm/h could trigger discharge responses in developed watersheds like Black Creek and the River des Peres. Fox Creek's flood behavior was characterized by the lowest peak discharges, slowest rising and falling limbs responses, and longest lag times of all the basins. Average lag times shortened as impervious surface area increased in the watersheds, decreasing from 4.8 h at Fox Creek to 1.3 h at Black Creek (Table 1). The relationship between impervious surface area and lag time was non-linear (Fig. 2A), with suburban Grand Glaize Creek exhibiting intermediate average lag times of 3.8 h (Table 1).

We used both specific conductivity and O isotopes for two-component hydrograph separations to quantify baseflow and event water contributions along the rural to urban land use gradient. Overall, there was good agreement between the two types of separation methods, and baseflow calculations were within ±5% for all measured storms (Table 1; Fig. 2B). Specific conductivity hydrograph separations were not performed for any sites from mid-December 2007 to mid-March 2008 due to the use of deicing chemicals. We also did not conduct specific conductivity separations for the River des Peres from mid-March 2008 to the end of our monitoring period in September 2008 because backwater from flooding on the Mississippi River affected the site. For comparison, Fig. 2B shows average baseflow contributions calculated by: (1) isotope hydrograph separations for the entire monitoring period, (2) specific conductivity hydrograph separations for the entire monitoring period (excluding the winter months when deicing chemicals were used), and (3) specific conductivity hydrograph separations for October to mid-December 2007 (before both road salting and backwater affected the River des Peres).

Both separations methods reveal that, on average, baseflow inputs during floods were reduced by ~40% when urban Black Creek (with 41.2% impervious surface area) is compared to rural Fox Creek (with 1.5% impervious surface area; Table 1; Fig. 2B). During the seasonally drier conditions in the fall of 2007, peak flows were lower and baseflow contributions were higher in all the streams (Fig. 2B). Nevertheless, the urban River des Peres still featured substantially lower baseflow inputs (i.e., an average of 27% less) compared to corresponding floods on Fox Creek. Interestingly, the trend of decreasing baseflow contributions as a function of increasing impervious surface area was not linear, similar to the relationship observed for lag time (Fig. 2). The average baseflow component was only ~10% lower at suburban Grand Glaize Creek compared to rural Fox Creek, despite nearly 25% more impervious surface area in the Grand Glaize Creek watershed. However, the average baseflow component during flooding at Grand Glaize Creek was >25% higher than Black Creek and ~20% higher than the River des Peres (for comparable storms in the fall of 2007), while the difference in impervious surface area between Grand Glaize Creek and the urban end-members is only ~15%. This same non-linear trend was observed for the rural to urban land use gradient when other land use metrics such as forest cover and development level were compared to percent baseflow.

Flood responses for the streams varied depending on rainfall amounts and antecedent moisture conditions. There was a positive correlation between new runoff (i.e., event water normalized to basin area) and total rainfall for all of the watersheds (Fig. 3A). The slope of new runoff versus total rainfall, which is a measure of the runoff efficiency, decreased with reduced impervious surface area in the watershed. Indeed, Black Creek's slope was closest to unity at 0.81, while Fox Creek's slope was 0.49 (Fig. 3A). For precipitation events of ≥1.5 cm, event water typically comprised >70% of the total discharge in urban Black Creek, though it often approached 100% near peak flow. In contrast, during discharge perturbations in rural Fox Creek, event water usually comprised about 40% of the total discharge, but could reach ~80% during large precipitation events. Overall baseflow contributions during floods decreased as peak flow (normalized for area) increased (Fig. 3B). Black Creek featured the highest average area-normalized peak flows and lowest baseflow, while Fox Creek had the lowest area-normalized peak flows and highest baseflow; Grand Glaize Creek demonstrated an intermediate signature. We also observed variable contributions of new runoff for storms with similar rainfall totals but differing antecedent moisture conditions. Flood events that were preceded by wetter periods often had a lower baseflow component. These differences were most pronounced in our rural end-member, where we observed as much as a four-fold increase in new runoff for similar rainfall totals due to differences in antecedent moisture conditions (Fig. 3A). In contrast, in urban Black Creek we observed little variability in events with similar rainfall totals, despite differences in antecedent moisture conditions.

The baseflow and event water component hydrographs for all of the streams exhibited characteristics common to the overall discharge hydrograph shape, including the slopes of rising and recessional limbs as well as the peak shape (Figs. 4 and 5A). Either component could dominate the total discharge signal depending on basin conditions, but as shown in Fig. 2B, baseflow contributions during floods decreased as impervious surface area in the watershed increased. During some floods, the slopes of individual discharge curves exhibited subtle differences due to changes in the

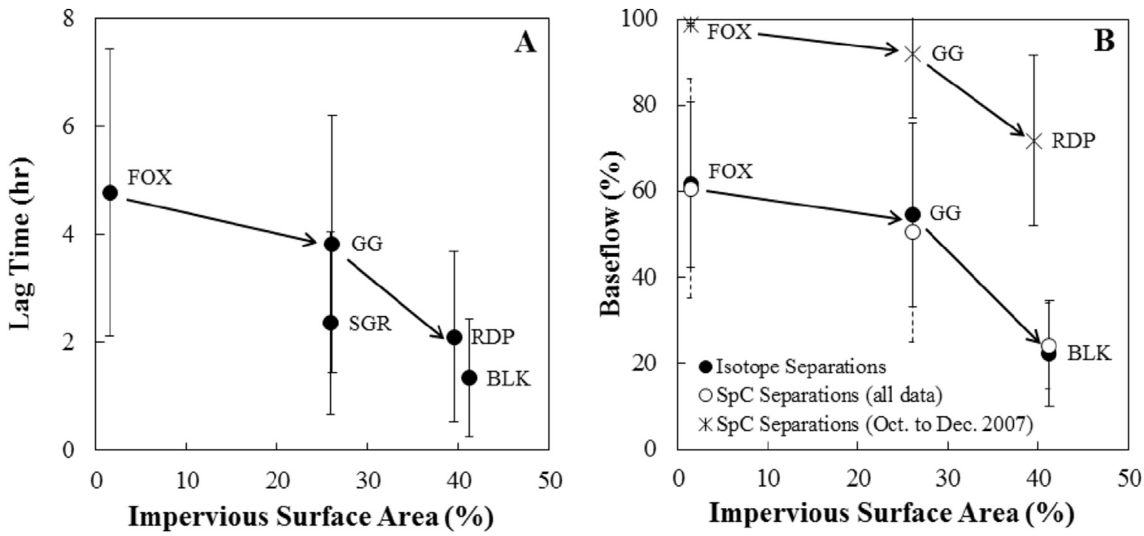

Fig. 2. Average lag times (A) and average percent baseflow contribution during floods (B) plotted against impervious surface area. Data for Fox Creek (FOX), Grand Glaize Creek (GG), Sugar Creek (SGR), the River des Peres (RDP), and Black Creek (BLK) are shown. In A, the standard deviations for lag times in each basin are given. In B, average baseflow percentages were calculated with either $\delta^{18}O$ (closed circles; standard deviation = solid lines) or specific conductivity (SpC; open circles; standard deviation = dashed lines; data from mid-December to mid-March are excluded due to applications of deicing chemicals) hydrograph separations. Because the River des Peres was affected by backwater from the Mississippi River from March to September 2008, a separate trend for specific conductivity separations from October to mid-December 2007 at Fox Creek, Grand Glaize Creek, and the River des Peres (asterisks; standard deviation = solid lines; note: the standard deviation for Fox Creek is smaller than the data point) is shown for comparison. These data were collected during a drier period that featured relatively small flood peaks in all the basins (see Fig. 6A). Therefore, all the streams had higher baseflow contributions. Both figures quantitatively illustrate that as urbanization increases in a watershed, so does the amount of physical variability.

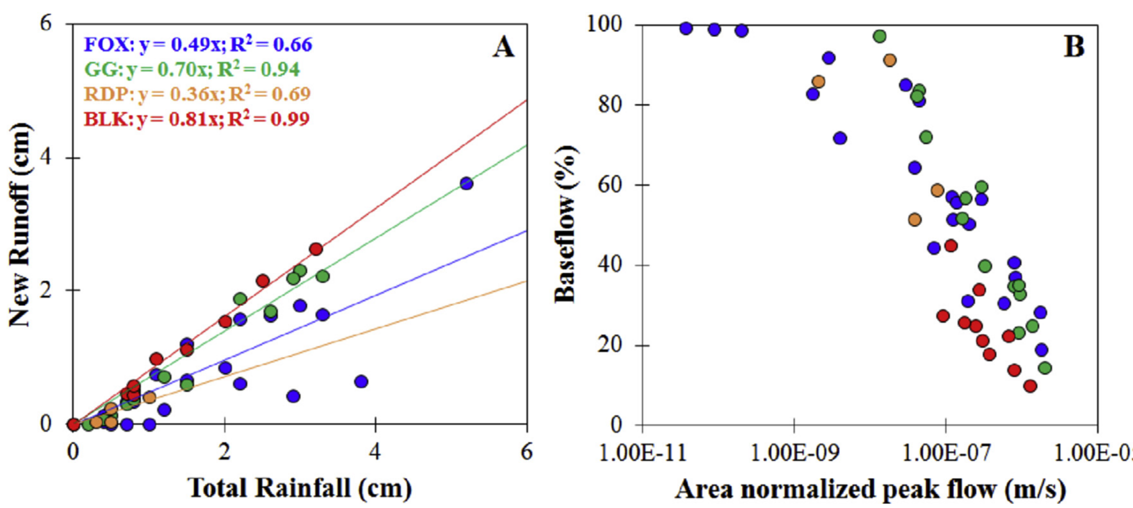

Fig. 3. New runoff (i.e., event water during floods normalized to basin area) plotted against total rainfall (NOAA, 2016) for individual precipitation events (A), and baseflow plotted against area-normalized peak flow (B). Data for Fox Creek (FOX; blue), Grand Glaize Creek (GG; green), the River des Peres (RDP; orange), and Black Creek (BLK; red) are shown. New runoff and baseflow values for the River des Peres were calculated only for the fall of 2007 when the site was not affected by backwater from the Mississippi River. In B, note that baseflow generally decreases as peak flow increases. Peak flow data are from USGS (2016). For interpretation of the references to color in this figure legend, the reader is referred to the web version of this article.

proportion of the flow components (Figs. 4 and 5A). Baseflow and event water hydrographs commonly rose together, but the timing of peak component discharge varied depending on antecedent moisture conditions and land use in the watershed. Event water in our urban end-member streams was usually delivered on the rising limb of the hydrograph prior to the baseflow component, peaking 15–30 min before the baseflow fraction. In our rural and suburban streams, baseflow was typically higher throughout the flood hydrograph and often peaked ~1 h before the event water peaked.

3.1.2. Individual flood responses across a rural to urban gradient

During the study period, we collected geochemical data for more than 50 storm-induced discharge perturbations at the study sites. We selected two rainfall events that occurred in April 2008 (Fig. 4) and May 2008 (Fig. 5) that led to considerable flooding at Fox Creek, Grand Glaize Creek, and Black Creek for detailed discussion here because both are representative of other flood responses in these basins. The April 2008 event represents a relatively simple, single hydrograph response for the basins, while the May 2008 event demonstrates how each basin responds to more complex precipitation events.

3.1.2.1. April 2008 flooding event. During the April 2008 event, rain fell mostly in one increment from 5:00–10:00 on April 3, delivering

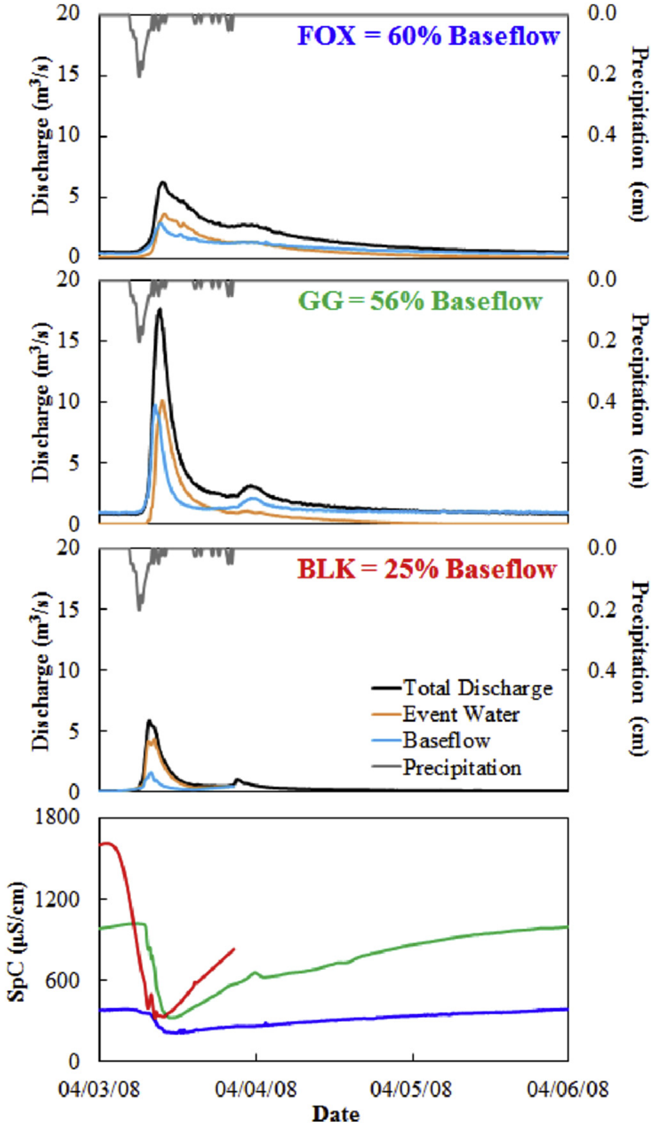

Fig. 4. The discharge and specific conductivity (SpC) responses for Fox Creek (FOX; blue), Grand Glaize Creek (GG; green), and Black Creek (BLK; red) during an April 3, 2008, rainfall event. Specific conductivity hydrograph separations demonstrate the decreasing baseflow contributions along the rural to urban transect for a single and relatively simple flood pulse. Variations in specific conductivity during the event increase and occur more rapidly as urbanization increases in the basins. All data are from this study except for the total discharge (USGS, 2016) and rainfall records (NOAA, 2016). For interpretation of the references to color in this figure legend, the reader is referred to the web version of this article.

a total of 1.52 cm (Fig. 4). Only 0.25 cm fell later that day over a 6 h period. A total of 4.34 cm of rain had fallen in the preceding 5 days. Only specific conductivity was measured for all three basins during this precipitation event and was used for the hydrograph separations (Fig. 4). During the event, Fox Creek had the most attenuated hydrologic response of all the basins. Peak discharge at this rural end-member reached 6.3 m^3/s approximately 4 h after the most intense rainfall. In comparison, Grand Glaize Creek had a peak flow of 17.6 m^3/s (more than twice that of Fox Creek when flow was normalized to basin area), which occurred 30 min before peak flow at the rural end-member. The discharge peak at urban Black Creek was 5.9 m^3/s; nearly the same peak flow as Fox Creek, despite having half the watershed area. Black Creek also had the most rapid response of all the monitored streams, and reached peak flow only 1.5 h after the most intense rainfall. The highest baseflow contribution using specific conductivity hydrograph separations was observed at Fox Creek (60%), but baseflow decreased with increasing urban land use to 56% at Grand Glaize Creek and 25% at Black Creek (Fig. 4). We also observed differences in the peak flow timing for the two flow components, with the baseflow fraction peaking before the event water fraction at Fox Creek (45 min prior) and Grand Glaize Creek (75 min prior), but the event water fraction peaking 30 min prior to the baseflow fraction at Black Creek.

The specific conductivity responses also featured shortened lag times and increased variability with increasing urban land cover (Fig. 4). Rural Fox Creek had the lowest pre-event specific conductivity value (384 µS/cm), followed by Grand Glaize Creek (1004 µS/cm), and then Black Creek (1559 µS/cm). The minimum specific conductivity values during the flood at Black Creek occurred 3.5 h earlier than at Fox Creek. Similarly, the magnitude of change in specific conductivity from pre-event values to minimum levels during the flood increased across our rural to urban gradient from a difference of 173 µS/cm at our rural site to 1238 µS/cm at our urban site.

3.1.2.2. May 2008 flooding event. The May 2008 event illustrates a more complex response in the three basins (Fig. 5). During this storm, rain fell in several distinct increments: 0.78 cm at 7:00 on May 7, 2.48 cm from 13:00–23:30 on May 7, 2.28 cm from 1:00–12:30 on May 8, and 0.20 cm from 9:30–11:00 on May 9, resulting in a total of 5.73 cm (Fig. 5A). A total of 0.48 cm of rain had fallen five days prior to the May 7–9 rainfall. Time series rain samples were collected for isotopic analysis from Washington and Saint Louis, Missouri. A composite sample of May 7–9 precipitation collected at Ladue, Missouri, had δD and $\delta^{18}O$ values of −32‰ and −5.4‰, which was approximately the same as the weighted average of the individual Saint Louis (−31‰ and −5.3‰) and Washington (−34‰ and −5.8‰) precipitation samples. For our isotope hydrograph separations, we used rainfall isotope compositions for the precipitation station nearest to the watershed of interest: at Fox Creek we used rainfall isotope data from Washington and at Grand Glaize Creek and Black Creek we used rainfall isotope data from Saint Louis. We did not use the Ladue rainfall isotope data for hydrograph separations because the sample was a composite and therefore could not be used for a detailed time series.

The rural end-member had the most attenuated physical and geochemical responses of the three watersheds to the May 2008 rainfall (Fig. 5). At Fox Creek, there were two low, broad discharge peaks with flows of only 5.7 m^3/s and 8.8 m^3/s, compared to peak flows in the other basins that increased in number, volume, and complexity as urbanization increased (Fig. 5A). Peak discharge reached 58.0 m^3/s at Grand Glaize Creek and, when normalized to basin area, was nearly five times higher than Fox Creek. Grand Glaize Creek also featured three hydrograph responses, all of which had shorter rising and falling limbs than the rural end-member. Black Creek had a total of four distinct hydrograph responses, including complex behavior following the second increment of rain. The largest peak flow at Black Creek (10.4 m^3/s) was ~20% higher than the highest peak observed at Fox Creek.

Fox Creek's isotopic response to the storm perturbations was minimal compared to the other basins (Fig. 5B). Baseflow was characterized by isotope values of −44‰ and −6.8‰, and the maximum excursion from these values (i.e., −39‰ and −6.1‰) was observed on the recessional limb of the second discharge peak. Isotope samples collected during peak discharge for the second event at Grand Glaize Creek reached a maximum value of −20‰ and −3.8‰, while Black Creek reached a maximum value of −12‰ and −3.0‰ (approaching the rainfall values of −9‰ and −2.3‰ for

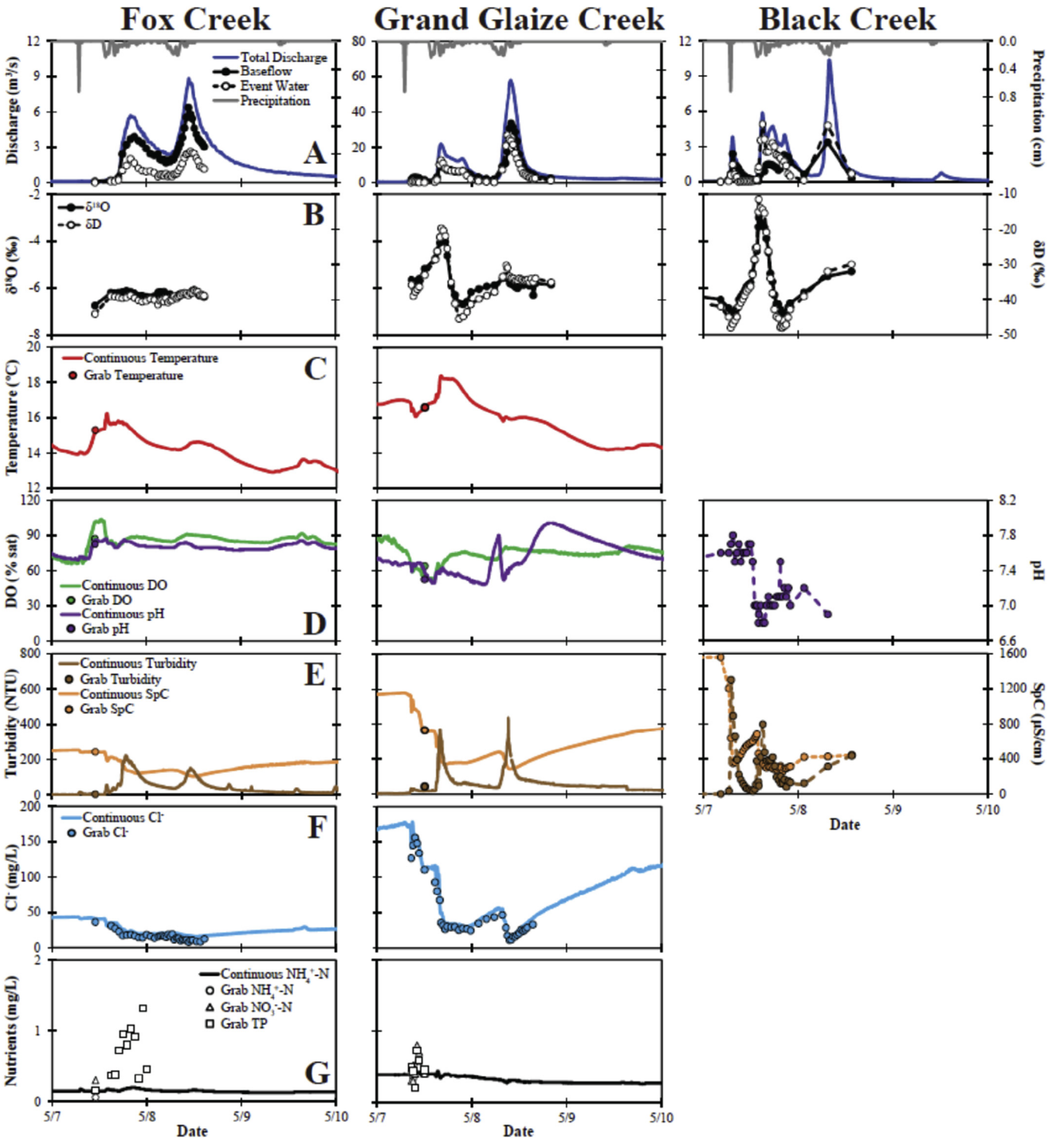

Fig. 5. The hydrologic, isotopic, and geochemical responses for Fox Creek, Grand Glaize Creek, and Black Creek during a May 7–9, 2008, rainfall event. Continuous monitoring data are shown as solid lines and point sampling data are shown as circles, triangles, or squares. Results include: (A) total discharge, baseflow and stormflow component hydrographs (determined by isotopic hydrograph separation; these values show good agreement with specific conductivity separations for these events, i.e., within 3%), and precipitation time series, (B) δD and $\delta^{18}O$ results, in situ and field measurements for (C) temperature, (D) DO and pH, and (E) turbidity and specific conductivity (SpC), and in situ and lab measurements of (F) Cl^- and (G) NH_4^+-N, NO_3^--N, and total P (TP). During this event, the continuous monitoring device at Black Creek malfunction, so only point measurements of pH, turbidity, and specific conductivity are shown. All parameters are on the same scale except for discharge at Grand Glaize Creek due to its large magnitude. All data are from this study except for the total discharge (USGS, 2016) and rainfall records (NOAA, 2016).

that period in the storm).

Over the May 2008 flooding events, temperature was, on average, 1.8 °C higher at Grand Glaize Creek than Fox Creek (Fig. 5C). A small temperature excursion (~0.7 °C) on the rising limb of the first discharge response at Fox Creek was superimposed on diurnal temperature variations. A temperature anomaly associated with the rising limb of the analogous flood hydrograph at Grand Glaize Creek was also observed, but the change was twice that of

Fox Creek. The DO responses at Fox Creek and Grand Glaize Creek were complex, with DO increasing at Fox Creek, but decreasing at Grand Glaize Creek in response to the second increment of rainfall (Fig. 5D). After these initial perturbations, DO at both sites remained relatively constant (i.e., ±3%). Overall variations in DO during the May events were similar between the two sites (i.e., ±7.2% for Fox Creek and ±7.0% for Grand Glaize Creek). In contrast, the variation in pH increased four-fold from Fox Creek (±0.05) to Grand Glaize Creek (±0.20), while Black Creek was most variable (±0.45; Fig. 5D). Like pH, the average turbidity values (Fig. 5E) rose with increasing urbanization. Peak turbidity in Fox Creek was 52% lower than Grand Glaize Creek and 67% lower than Black Creek. Additionally, the onset of the turbidity peak was shortened in urban Black Creek by 15–30 min compared to the less urbanized basins.

During the floods, specific conductivity decreased by 58%, 76%, and 84% for Fox Creek, Grand Glaize Creek, and Black Creek, respectively (Fig. 5E). This response was typical of the streams, and specific conductivity underwent significant reduction during the rising limb of the hydrograph, commonly around 50% for the rural stream and up to 95% for the suburban and urban streams. The Cl^- concentrations mirrored the specific conductivity behavior, but the overall reduction in Cl^- concentrations was higher, with a 75% reduction at Fox Creek and 93% reduction at Grand Glaize Creek (Fig. 5F). Fox Creek's NH_4^+-N concentrations remained relatively constant (about 0.2 mg/L) throughout the perturbation, while total P increased more than 1 mg/L. Like Fox Creek, NH_4^+-N concentrations at Grand Glaize Creek remained steady during the monitoring period, but were about 0.3 mg/L higher. The NO_3^--N concentration increased from 0.3 mg/L to a maximum of 0.8 mg/L during the first flooding event at Grand Glaize Creek. The highest total P concentration at Grand Glaize Creek was half that of Fox Creek (Fig. 5G).

3.2. Seasonal stream response across a rural to urban gradient

Seasonal variations in streamflow and geochemistry from October 2007 to September 2008 are given in Table 2, Fig. 6, and Fig. 7, and demonstrate increasing variability in nearly every geochemical parameter as impervious surface area in the basins increased. Small gaps in the dataset are due to occasional equipment malfunctions or when the sites were affected by backwater. Geochemical data for the River des Peres after March 3, 2008, have been excluded because the site was affected by prolonged backwater from flooding on the Mississippi River. Samples from Black Creek were collected from March to September 2008.

Variability of seasonal discharge increased across the rural to urban gradient (Fig. 6A), with Fox Creek having a standard deviation for discharge of 0.8 m^3/s compared to 7.1 m^3/s and 3.2 m^3/s at the River des Peres and Black Creek, respectively (Table 2). Predictably, as air temperature decreased in the winter months, water temperatures decreased in the continuously monitored basins (Fig. 6B). Fox Creek's seasonal temperature response was attenuated compared to the other watersheds (standard deviation = 3.8 °C), while the River des Peres had the most extreme temperature changes (standard deviation = 5.2 °C; see continuous monitoring data in Table 2). Water temperatures at Fox Creek never reached freezing and the coldest temperature measured there was 1.3 °C. This minimum occurred after a prolonged cold period when the average air temperature had been -5 °C during the preceding week. Grand Glaize Creek exhibited larger temperature variations (standard deviation = 4.4 °C; Table 2) than Fox Creek, and reached 0 °C several times during the winter (Fig. 6B). The temperature of grab samples from Grand Glaize Creek's subbasin, Sugar Creek, were on average 1.7 °C lower than grab samples from Grand Glaize Creek (Table 2). Freezing water temperatures were observed at the River des Peres many times during January and February of 2008. Moreover, the River des Peres' water temperature often changed by >5 °C per day over the entire monitoring period (Fig. 6B). Because temperature at Black Creek was measured from March to September 2008, we are not able to compare these data to the other sites.

Area-normalized DO loads were two to five times higher in the suburban and urban streams compared to the rural stream (Table 2). There were significant (>50%) diurnal oscillations in DO at all the sites, with the highest DO values observed in the mid-afternoon and the lowest values observed in the early morning. The amplitude of these changes increased with increasing impervious surface area in the basin (Fig. 6C). The average pH was largely circumneutral for all the sampling locations, but, like DO, also increased as urban land use increased in the basin (Table 2). Fox Creek and Grand Glaize Creek had more attenuated flood, diurnal, and seasonal pH variations than the River des Peres (Fig. 6D). For example, the River des Peres exhibited pH variations of up to 3.5 units (reaching maximum values of 11) associated with floods. Like DO, diurnal variations at the sites featured high pH during the mid-afternoon and low pH during the early morning hours, with the largest variations observed at the River des Peres (up to 1 pH unit) in fall and winter of 2007. The highest turbidity levels for all the streams were observed on the rising limb of discharge pulses (Fig. 6E). Periodically, continuously monitored turbidity at Fox Creek increased for a single data point. Nevertheless, turbidity grab sample data was lowest for Fox Creek and increased three- to 50-fold in the suburban and urban streams (Table 2).

The average specific conductivity was lowest at Fox Creek, followed by the River des Peres and its subbasin Black Creek, with Grand Glaize Creek and its subbasin Sugar Creek featuring the highest specific conductivity (Table 2). Continuous monitoring data show periods of high specific conductivity were associated with road salt application: predictably, high specific conductivity coincided with high Cl^- levels (Fig. 6F and G, respectively). Moreover, these spikes in Cl^- concentration were consistently higher than the USEPA limit for chronic Cl^- contamination (230 mg/L) during the winter, and on several occasions exceeded the acute level (860 mg/L; Fig. 6G). While Fox Creek had the lowest Cl^- loads, surprisingly, Cl^- loads were the highest in the Grand Glaize Creek watershed rather than the River des Peres basin (i.e., Cl^- loads did not correlate with increasing impervious surface area in the watersheds). Nutrient (i.e., NH_4^+-N, NO_3^--N, and total P) load averages and standard deviations increased exponentially with increasing impervious surface area (Table 2; Fig. 6H). Similarly, bacterial loads (i.e., *E. coli*) also increased exponentially with increasing impervious surface area (Table 2). However, the variability of $\delta^{18}O$ increased linearly with increasing impervious surface (Fig. 7).

4. Discussion

Discharge and geochemical data from the five watersheds along our rural to urban land use gradient in Saint Louis, Missouri, clearly show that as impervious surface area increases in the basins so does the variability in both the hydrological and geochemical responses of streams. Component hydrographs reveal that the relative contribution of pre-event water to streamflow during flooding decreases as urban land use increases. Notably, this behavior is not linear, indicating that the hydrology of suburban watersheds is less impacted than might be predicted by their land use and land cover. Individual chemical constituents in streamflow also show that short-term (i.e., flooding and diurnal) and long-term (i.e., seasonal) geochemical variability generally increased as a function of land use, and this relationship can be either linear or non-linear. Here, we interpret both component hydrograph and geochemical responses across our rural to urban land use gradient.

Table 2
Average values, standard deviations (StDev), number of samples (n), and area-normalized loads for various physical, geochemical, and bacterial parameters at the stream sites. Both continuous monitoring and grab sample data are presented; all data are for October 2007 to March 2008, except for Black Creek, for which the data range is from March to September 2008.

Site	Measurement	Statistical Analysis[a]	Discharge (m^3/s)	$\delta^{18}O$ (‰)	Temperature (°C)	DO (%)	DO (mg/L)	pH	Turbidity (NTU)	SpC (uS/cm)	Cl^- (mg/L)	NH_4^+-N (mg/L)	NO_3^--N (mg/L)	TP (mg/L)	*E. coli* (cfu/100 mL)[b,c]
Fox Creek	Continuous	Average	0.1	NA	7.2	64.5	8.0	7.4	10	896	170.1	0.35	NA	NA	NA
		StDev	0.8	NA	3.8	23.2	3.2	0.2	51	680	260.9	0.20	NA	NA	NA
		n	12,897	NA	36,362	36,362	36,362	36,362	36,362	36,362	36,362	21,470	NA	NA	NA
		Load	NA	NA	NA	NA	2.1	NA	NA	NA	45.2	0.09	NA	NA	NA
	Grab	Average	0.1	−6.5	7.9	73.4	8.9	6.9	3	693	73.0	0.09	0.84	0.23	21.6
		StDev	0.8	0.3	4.1	20.1	3.0	0.4	3	68	14.8	0.06	0.50	0.17	39.5
		n	12,897	10	10	10	10	10	10	10	10	10	10	10	10 (0%)
		Load	NA	NA	NA	NA	2.4	NA	NA	NA	19.4	0.02	0.22	0.06	6
Grand Glaize Creek	Continuous	Average	0.4	NA	5.4	78.1	10.0	7.7	19	1575	505.6	0.46	NA	NA	NA
		StDev	2.5	NA	4.4	19.9	3.3	0.2	75	1558	756.7	0.47	NA	NA	NA
		n	39,791	NA	36,670	36,670	36,670	36,670	36,670	36,670	36,670	36,670	NA	NA	NA
		Load	NA	NA	NA	NA	6.0	NA	NA	NA	306.2	0.28	NA	NA	NA
	Grab	Average	0.4	−6.8	6.8	85.5	10.6	7.1	17	2023	498.4	0.20	1.40	0.34	553.9
		StDev	2.5	1.0	4.5	23.0	3.5	0.3	15	2265	682.2	0.10	0.40	0.15	773.0
		n	39,791	10	10	10	10	10	10	10	10	10	10	10	10 (0%)
		Load	NA	NA	NA	NA	6.4	NA	NA	NA	301.8	0.12	0.85	0.21	335
Sugar Creek	Grab	Average	0.1	−6.7	5.1	103.2	13.2	7.2	9	2281	525.3	0.14	1.16	0.24	274.6
		StDev	0.7	1.0	2.2	18.0	3.0	0.2	7	1516	484.1	0.08	0.85	0.17	453.8
		n	34,223	8	9	9	9	9	9	9	9	9	9	9	9 (0%)
		Load	NA	NA	NA	NA	7.7	NA	NA	NA	307.1	0.08	0.68	0.14	161
River des Peres	Continuous	Average	1.6	NA	6.1	83.7	10.4	8.0	14	1178	372.0	1.20	NA	NA	NA
		StDev	7.1	NA	5.2	21.4	2.6	0.5	28	1124	588.4	0.77	NA	NA	NA
		n	39,828	NA	37,186	37,186	37,186	37,186	37,186	37,186	37,186	37,186	NA	NA	NA
		Load	NA	NA	NA	NA	4.7	NA	7	NA	169.8	0.55	NA	NA	NA
	Grab	Average	1.6	−7.2	8.7	90.7	10.7	7.6	64	786	62.0	0.89	2.12	0.65	726.9
		StDev	7.1	1.0	5.1	17.8	2.6	1.0	100	280	68.9	0.78	0.88	0.41	1189.3
		n	39,828	10	11	11	11	10	10	11	11	11	11	10	11 (36%)
		Load	NA	NA	NA	NA	4.9	NA	NA	NA	28.3	0.40	0.97	0.30	332
Black Creek	Grab	Average	0.4	−6.0	23.5	78.3	7.2	7.6	150	656	194.0	0.21	3.6	0.43	1732.9
		StDev	3.2	1.4	4.4	11.1	1.6	0.5	220	418	NA	NA	NA	NA	NA
		n	55,194	241	82	8	8	141	241	241	1	1	1	1	1 (0%)
		Load	NA	NA	NA	NA	12.4	NA	NA	NA	333.3	0.36	6.19	0.74	2978

NA = not applicable.
[a] All stream load values are area-normalized and in units of $kg/day/km^2$, with the exception of *E. coli* loads, which are in units of 1,000,000 $cfu/day/km^2$.
[b] Most probable number range: 1–2,420 cfu/100 mL.
[c] Obtaining an average was not always possible due to off-scale measurements; the percentage of measurements that were off-scale is given in parentheses next to the sample n values.

4.1. *Natural hydrological response is altered by urbanization*

High flow conditions in streams represent the combined and rapid delivery of both baseflow and event water components. Event water mostly travels along surficial or transient shallow flowpaths and can constitute a significant portion of the total discharge during a storm pulse (Konrad, 2003; Vicars-Groening and Williams, 2007; Hasenmueller and Robinson, 2016). Previous observations have demonstrated that urban land use can lead to significant modification of stream flood response, including higher peak flows, shortened hydrograph responses, and higher event water contributions than their undisturbed counterparts (Arnold and Gibbons, 1996; Gremillion et al., 2000; Buda and DeWalle, 2009; Burns et al., 2012; Klaus and McDonnell, 2013). However, there has been no systematic assessment of stream flooding behavior along a rural to urban gradient to understand rainfall-runoff patterns and pollutant transport as a function of land use.

Like previous studies (e.g., Buttle et al., 1995; Gremillion et al., 2000; Buda and DeWalle, 2009; Meriano et al., 2011), we found that as impervious surface area in a watershed increases, so does the event water component of the hydrograph. However, our evaluation of baseflow and event water contributions during floods showed that the relationship between baseflow inputs and impervious surface area in the watersheds was not linear (Fig. 2B). Instead, the suburban stream in our study had baseflow inputs that were more similar to the rural end-member than the urban end-member, despite having intermediate impervious surface area (Table 1). The same non-linear trend was also observed when other land use attributes (e.g., forest cover and development level) were compared to percent baseflow. This suggests that while impervious surface area can dramatically increase the event water component in highly urbanized watersheds, suburban basins may be less impacted than predicted by land cover.

Lag times across the rural to urban gradient also had a non-linear relationship with impervious surface area (Fig. 2A), indicating that flow delivery during floods is slower in the suburban watershed than might be suggested by land use factors. We observed shorter average lag times in Grand Glaize Creek's subbasin Sugar Creek as well as the River des Peres' subbasin Black Creek (Fig. 2A). Faster flood responses in smaller watersheds compared to larger watersheds have been observed elsewhere (Dingman, 2002; Marchi et al., 2010). However, it is unlikely that differences in basin area caused higher baseflow inputs in the suburban watershed because we observed the same non-linear trend between baseflow and impervious surface area when Grand Glaize Creek was compared to the more urban River des Peres and its much smaller subbasin Black Creek. Basin soils and geology are also very similar between these watersheds, especially the suburban and urban basins (Lutzen and Rockaway, 1989; Harrison, 1997), and are therefore also an improbable cause of the non-linear trend

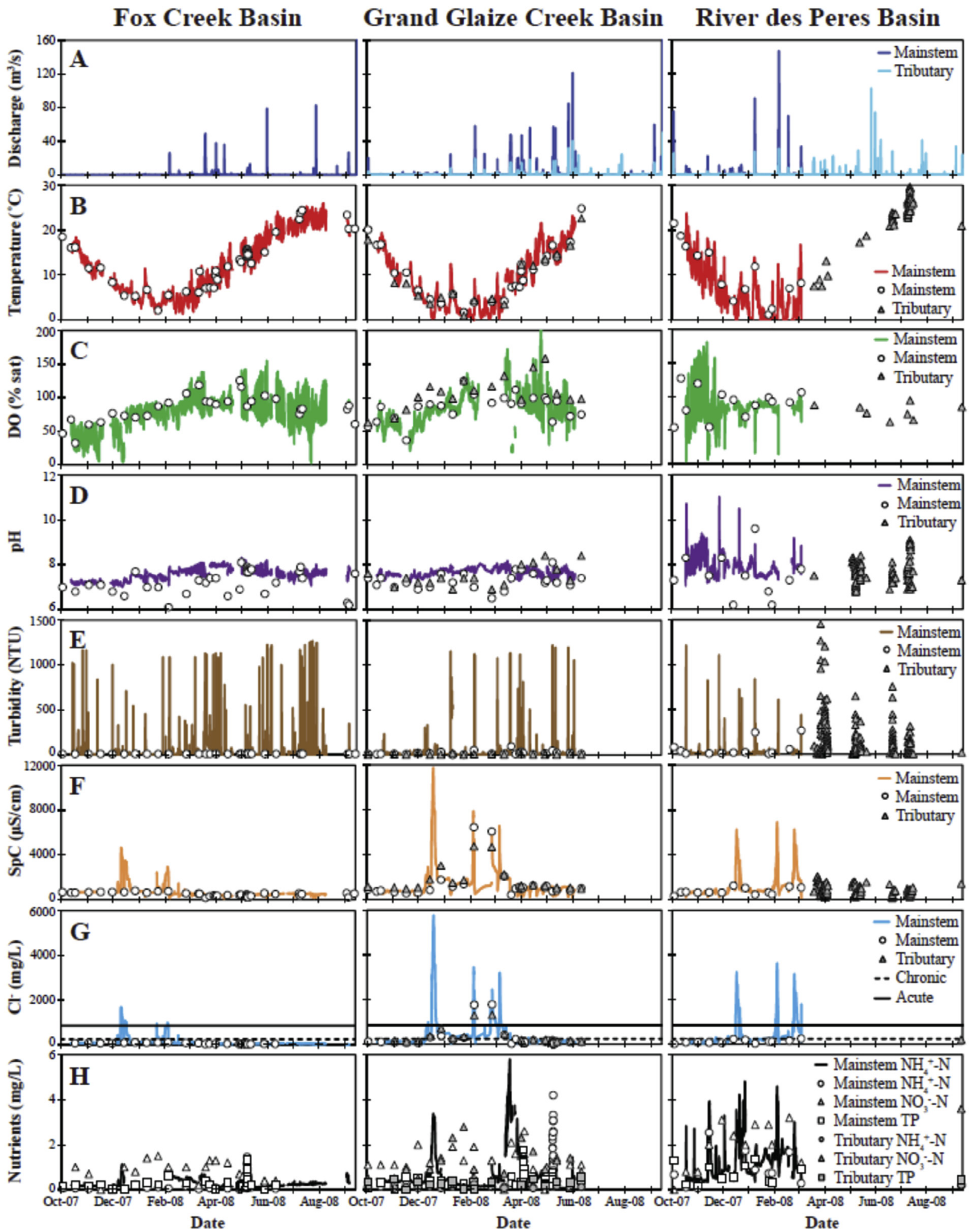

Fig. 6. Continuous monitoring (solid lines) and point sampling (open circles or shaded triangles) data for Fox Creek, Grand Glaize Creek, Sugar Creek, the River des Peres, and Black Creek from October 2007 to September 2008. Data for tributaries (i.e., Sugar Creek and Black Creek) are plotted with the mainstem streams (i.e., Grand Glaize Creek and the River des Peres, respectively). Results include: (A) total discharge, (B) temperature, (C) DO, (D) pH, (E) turbidity, (F) specific conductivity (SpC), (G) Cl^-, and (H) NH_4^+-N, NO_3^--N, and total P (TP). Gaps in the continuous monitoring data represent periods when sensors were damaged or backwater affected the sites. In our continuous monitoring data for Fox Creek, we observed that turbidity (E) would often increase for a single data point during low flow conditions. We suspect these short intervals of high turbidity were the result of a crayfish, which lived in the housing unit for the continuous monitoring device, moving over the sensors. The USEPA's chronic (230 mg/L) and acute (860 mg/L) Cl^- contamination levels are plotted on the Cl^- diagrams (G) for reference.

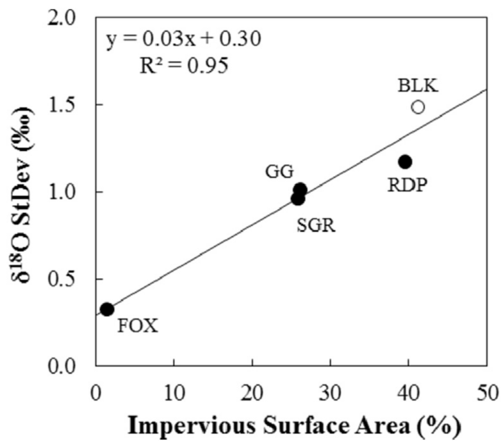

Fig. 7. The variability (i.e., standard deviation; StDev) of $\delta^{18}O$ in stream samples plotted against impervious surface area in Fox Creek (FOX), Grand Glaize Creek (GG), Sugar Creek (SGR), the River des Peres (RDP), and Black Creek (BLK). The standard deviations of $\delta^{18}O$ measurements overlap in time (i.e., October 2007 to March 2008) for points with closed circles, while the values for Black Creek are shown as an open circle because these data were collected from March to September 2008 (see Table 2). The figure quantitatively illustrates that as urbanization increases in a watershed, so does the amount of geochemical variability.

in baseflow as a function of land use. Further study is needed to determine why baseflow inputs as well as the delivery of water (i.e., lag times) demonstrate non-linear relationships with increasing urbanization.

Individual flood responses for each basin varied depending on rainfall amounts and antecedent moisture conditions (Fig. 3). New runoff in the streams generally increased with increasing total rainfall volumes (Fig. 3A), but this behavior could be confounded by storms that occurred prior to the event of interest. Winston (2001) and Winston and Criss (2004) extensively document that the magnitude and timing of discharge and specific conductivity variations in a karst spring, located along the same transect as this study between the Fox Creek and Grand Glaize Creek basins, were impacted by the separation between storm events. Long periods of dry conditions tended to reduce discharge peaks and specific conductivity excursions, but frequent storms "primed" the basin to respond more and led to dramatic specific conductivity excursions, higher peak flows, and greater event water contributions. Surprisingly, we observed the most variability in new runoff due to antecedent moisture conditions in our rural end-member, Fox Creek. Higher variability in new runoff volumes in our rural end-member compared to the suburban and urban streams suggests that urban land cover limits the effect of antecedent moisture conditions. Indeed, less soil cover in suburban and urban watersheds would decrease the ability of frequent rainfall events to saturate soils (thereby reducing infiltration rates) and "prime" the basins.

Event water in our urban end-member streams was generally delivered prior to the baseflow component (Figs. 4 and 5), a result of the rapid transfer of surface runoff into these systems. However, baseflow was generally delivered before event water in both the rural and suburban streams. Baseflow delivery dominated the rising limb of the hydrograph at Fox Creek and Grand Glaize Creek because higher infiltration rates hydraulically force baseflow into the streams (Dingman, 2002).

4.2. Geochemical response to urbanization

4.2.1. Hierarchy of transport timescales during flood response

During flooding events, different water quality parameters along our rural to urban gradient responded over different timescales (Figs. 4 and 5). Winston and Criss (2004) also showed that different physical and geochemical parameters have a hierarchy of transport timescales. When analogous flooding events are compared, the most rapidly responding constituents for all the basins were turbidity, temperature, DO, and pH, followed by specific conductivity and Cl^-, then the nutrients NO_3^--N and total P. Importantly, urbanization generally shortened the transport timescales and enhanced the variability of each of these individual parameters relative to our rural end-member. Moreover, the transport timescales of measured constituents in all of the streams were shorter than those observed for a nearby karst spring system, which often featured response times that were >50% longer than our rural end-member stream (Winston and Criss, 2004). Transport of suspended sediment, as characterized by the turbidity, increased substantially due to intensifying flood severity caused by urbanization. Sharp perturbations of turbidity, as well as temperature, DO, and pH, correlated most closely with the event water fraction. For example, temperature variations were amplified by increased urban land coverage, and could differ from their rural counterparts by 2 °C or more, depending on the event water temperature. The lag to the peak change in turbidity, temperature, DO, or pH was shortened as impervious surface area increased in the basin. Indeed, when compared to Fox Creek, turbidity values peaked during flood events by as much as 2.5 h earlier at Grand Glaize Creek and 3.5 h earlier at Black Creek, though timing varied depending on the flood event.

Minimum specific conductivity invariably followed the discharge maximum in rural Fox Creek, typically by more than 1 h and roughly corresponded to the point where the volumetric event water contribution reached a fractional maximum relative to the baseflow component. However, in urban environments, like Black Creek, minimum specific conductivity followed the discharge peak typically by only 30 min, and in some cases was concurrent with the peak (Figs. 4 and 5E). Recovery to pre-event specific conductivity levels occurred slowly, and usually lagged behind the loss of the event water component, indicating the variable nature of baseflow specific conductivity, a feature also observed by Winston and Criss (2004).

During the onset of a flood event, specific conductivity could exhibit complex behavior including significant positive or negative variations (Figs. 4 and 5E), and these fluctuations were superimposed on the general dilution curve associated with discharge events (cf. Winston, 2001; Winston and Criss, 2004; Pellerin et al., 2008). These variations were caused by different proportions of the individual flow components, and were observed when the event water contribution began to increase relative to baseflow. A reversal of the dilution trend took place when the event water component began to crest and baseflow was still rising or cresting at a slower rate. The reduction in specific conductivity resumed when delivery of the baseflow component underwent a rate change and began to decline more rapidly than the event water component. All of the observed pulses in the basins showed transient minima in the specific conductivity dilution (Figs. 4 and 5E), and these minima always accompanied a change in the slope of the event water component. However, these variations increased in frequency and magnitude with increasing impervious surface area and could be due to the delivery of large event water components via storm sewers in the suburban and urban watersheds. At both Fox Creek and Grand Glaize Creek, NO_3^--N and total P concentrations typically peaked about 15–20 min after specific conductivity reached its minimum level (Fig. 5G). These nutrients were generally lower at Grand Glaize Creek during floods than Fox Creek, possibly because of the mobilization of nutrients from agricultural areas in the Fox Creek watershed following precipitation events.

4.2.2. Seasonal variations

Seasonal water quality data also demonstrate generally increasing variability in stream geochemistry as a function of increasing impervious surface area (Figs. 6 and 7). Indeed, variability in water temperature increased with urban land use (Table 2). Fox Creek never froze due to higher baseflow inputs reducing both daily and seasonal temperature oscillations. This is confirmed by our hydrograph separations (Fig. 2B) and the low variability of $\delta^{18}O$ in stream water (Fig. 7), both of which indicate high baseflow additions. In contrast, the River des Peres often experienced freezing temperatures in January and February 2008. Moreover, water temperatures at the River des Peres often changed by > 5 °C per day (Fig. 6B), confirming a very low baseflow component in this urban watershed.

Interestingly, a positive correlation existed between DO and impervious surface area (Table 2), and area-normalized DO loads were two to five times higher in the urban end-members compared to Fox Creek. This difference is likely due to eutrophication in the urban streams, with algal blooms increasing dissolved O_2 near the water surface. This was confirmed by high daily oscillations in DO for the urban catchment (Fig. 6C), which tended to be most variable during the early fall months when algae were more active. High pH in the River des Peres may also be due in part to eutrophication as algae remove CO_2 from the water column and subsequently increase pH. This is supported by large, daily oscillations of pH (up to 1 pH unit), especially in the warmer months (Fig. 6D). We also observed increasing acidity of stream waters with decreasing impervious surface area (Table 2), which may be due to higher soil water contributions in the less developed watersheds. The reason for large changes in pH during stormflow (i.e., >3 units) in the River des Peres is unclear, but may be associated with CSOs events.

We observed the lowest average turbidity values at Fox Creek (Table 2). Lower turbidity at the River des Peres compared to Grand Glaize Creek is likely due to cement-lined channels along this reach of the River des Peres, which restrict sediment supply (Hasenmueller and Robinson, 2016). Indeed, Black Creek, which has fewer channel linings than the River des Peres, had average turbidity levels that were almost three times higher than the River des Peres (Table 2), indicating that high flows in urban streams can mobilize and transport more sediment than their rural counterparts. Periodically, continuously monitored turbidity at Fox Creek increased for a single data point (Fig. 6E). We suspect these short intervals of high turbidity were the result of a crayfish, which lived in the housing unit for the continuous monitoring device, moving over the sensors.

Like turbidity, other water quality parameters did not increase with urbanization. Both specific conductivity and Cl^- were lowest in Fox Creek, followed by the urban end-members, then the suburban end-members (Table 2; Fig. 6F and G). Typically, Cl^- concentrations in streams have been observed to increase with urbanization because of the higher road densities in urban areas (Kaushal et al., 2005). However, we believe the high Cl^- values at Grand Glaize Creek are the result of higher road salt application rates per unit area in this watershed compared to the more urbanized River des Peres watershed. The average Cl^- concentration in Grand Glaize Creek is 35% higher than the River des Peres, yet the Grand Glaize Creek catchment has a lower road density than the River des Peres catchment. Therefore, higher Cl^- content at Grand Glaize Creek cannot simply be due to more road area impacted by salt application. This suggests that road salt application rates per unit length of road are higher in the Grand Glaize Creek basin compared to the River des Peres basin. Thus, while baseflow delivery during storms may be less impacted in suburban watersheds, these catchments may be more impaired for specific water quality parameters than predicted by their land cover. Nevertheless, all the monitored streams were impaired for Cl^-, including rural Fox Creek (Fig. 6G).

Unlike specific conductivity and Cl^- levels, nutrient levels increased along the rural to urban land use gradient, and this increase was exponential for NH_4^+-N, NO_3^--N, and total P. This relationship differs from our observations during flood events, when Fox Creek often had higher nutrient levels than Grand Glaize Creek (e.g., Fig. 5G). This indicates that while Fox Creek has low nutrient loads during low flow conditions, rainfall responses can rapidly mobilize nutrients in the basin, possibly from agricultural areas.

5. Conclusions

Watersheds along a rural to urban transect provide unique data that elucidate several significant and fundamental findings about the effect of land use on stream hydrology and geochemistry. Compared to their rural counterparts, floods on urban streams have: sharp rising and falling limbs, shorter lag times that are commonly <1.5 h, peak flows that are up to 10 times higher, short recession times, and much smaller baseflow fractions (by up to 40%). These features of urban streams are clearly related to their high impervious area, but a linear relationship was not observed between increasing impervious surface area and decreasing baseflow inputs. Thus, baseflow contributions in suburban watersheds may be less impacted than would be suggested by their impervious area. Additionally, water quality in streams generally became increasingly impacted and more variable as urban land use increased, as demonstrated by amplified variations in geochemistry on short-term and seasonal timescales. These geochemical variations demonstrate both linear and non-linear increases as a function of impervious surface area. Therefore, suburban watersheds may exhibit more or less water quality impairment than might be predicted by catchment land use. Collectively, the large variations in the physical and geochemical character of urban streams have negative consequences to environmental quality and aquatic life.

Acknowledgments

We thank those who helped with the field work and lab analyses, especially Lara Bennett, Kelson Hedderich, and Dwight McCay. Jeremy Fine is thanked for his help with GIS analyses, and Trish Reilly provided helpful guidance for field sample design. This work was partially supported by a USEPA subcontract from the Watershed Management Plan Development Grant Program through the Missouri Department of Natural Resources to the Saint Louis County Health Department (grant number G07-NPS-10).

References

American Society of Civil Engineers, 2016. River des Peres Sewage and Drainage Works. American Society of Civil Engineers Web page. http://www.asce.org/.
Alley, W.M., Veenhuis, J.E., 1983. Effective impervious area in urban runoff modeling. J. Hydraulic Eng. 109, 313–319.
Arnold Jr., C.L., Gibbons, C.J., 1996. Impervious surface coverage: the emergence of a key environmental indicator. J. Am. Plan. Assoc. 62, 243–258.
Borah, D.K., Bera, M., Shaw, S., 2003. Water, sediment, nutrient, and pesticide measurements in an agricultural watershed in Illinois during storm events. Trans. Am. Soc. Agric. Eng. 46, 657–674.
Brabec, E., Schulte, S., Richards, P.L., 2002. Impervious surfaces and water quality: a review of current literature and its implications for watershed planning. J. Plan. Literature 16, 499–514.
Brown, V.A., McDonnell, J.J., Burns, D.A., Kendall, C., 1999. The role of event water, a rapid shallow flow component, and catchment size in summer stormflow. J. Hydrol. 217, 171–190.
Buda, A.R., DeWalle, D.R., 2009. Dynamics of stream nitrate sources and flow pathways during stormflows on urban, forest and agricultural watersheds in central Pennsylvania, USA. Hydrol. Process. 23, 3292–3305.
Burns, M.J., Fletcher, T.D., Walsh, C.J., Ladson, A.R., Hatt, B.E., 2012. Hydrologic shortcomings of conventional urban stormwater management and opportunities for reform. Landsc. Urban Plan. 105, 230–240.

Buttle, J.M., Sami, K., 1992. Testing the groundwater ridging hypothesis of streamflow generation during snowmelt in a forested catchment. J. Hydrol. 135, 53–72.
Buttle, J.M., Vonk, A.M., Taylor, C.H., 1995. Applicability of isotopic hydrograph separation in a suburban basin during snowmelt. Hydrol. Process. 9, 197–211.
Corbett, K.T., 1997. Draining the metropolis: the politics of sewers in nineteenth century Saint Louis. In: Hurley, A. (Ed.), An Environmental History of Saint Louis. Missouri Historical Society, Saint Louis, pp. 107–125.
Criss, R.E., 1999. Principles of Stable Isotope Distribution. Oxford University Press, Oxford, p. 254.
Dingman, S.L., 2002. Physical Hydrology. Upper Saddle River, New Jersey, USA. Prentice Hall, p. 633.
Endreny, T.A., 2005. Land use and land cover effects on runoff processes: urban and suburban development. In: Anderson, M.G. (Ed.), Encyclopedia of Hydrological Sciences. John Wiley & Sons, Chichester, England, pp. 1775–1804.
Genereux, D.P., Hooper, R.P., 1998. Oxygen and hydrogen isotopes in rainfall-runoff studies. In: Kendall, C., McDonnell, J.J. (Eds.), Isotope Tracers in Catchment Hydrology. Elsevier, Amsterdam, pp. 319–346.
Gremillion, P., Gonyeau, A., Wanielista, M., 2000. Application of alternative hydrograph separation models to detect changes in flow paths in a watershed undergoing urban development. Hydrol. Process. 14, 1485–1501.
Hach, 2005a. Method 8206: Chloride, Mercuric Nitrate, in Digital Titrator Model 16900 Manual. Hach Company, pp. 67–68.
Hach, 2005b. Method 8038: Nitrogen, Ammonia: Nessler Method. Hach Company, pp. 1–6.
Hach, 2005c. Method 10020: Nitrate: Chromotrophic Acid Method. Hach Company, pp. 1–4.
Hach, 2005d. Method 8048: Phosphorus: Reactive (Orthophosphate) Method. Hach Company, pp. 1–6.
Hach, 2005e. Method 8190, Phosphorus: Total Digestion. Hach Company, pp. 1–4.
Hasenmueller, E.A., Criss, R.E., 2013. Geochemical techniques to discover open cave passage in karst spring systems. Appl. Geochem. 29, 126–134.
Hasenmueller, E.A., Robinson, H.K., 2016. Hyporheic zone flow disruption from channel linings: implications for the hydrology and geochemistry of an urban stream, Saint Louis, Missouri, USA. J. Earth Sci. 27, 98–109.
Harrison, R.W., 1997. Bedrock Geologic Map of the Saint Louis 30' × 60' Quadrangle, Missouri and Illinois. U.S. Geological Survey Miscellaneous Investigation Series Map I-2533, scale 1, p. 100,000.
Heppell, C.M., Chapman, A.S., 2006. Analysis of a two-component hydrograph separation model to predict herbicide runoff in drained soils. Agric. Water Manag. 79, 177–207.
Jefferson, A.J., Bell, C.D., Clinton, S.M., McMillan, S.K., 2015. Application of isotope hydrograph separation to understand contributions of stormwater control measures to urban headwater streams. Hydrol. Process. 29, 5290–5306.
Jennings, D.B., Jarnagin, S.T., 2002. Changes in anthropogenic impervious surfaces, precipitation and daily streamflow discharge: a historical perspective in a Mid-Atlantic subwatershed. Landsc. Ecol. 17, 471–489.
Kaushal, S.S., Groffman, P.M., Likens, G.E., Belt, K.T., Stack, W.P., Kelly, V.R., Band, L.E., Fisher, G.T., 2005. Increased salinization of fresh water in the northeastern United States. Proc. Natl. Acad. Sci. 102, 13517–13520.
Kaushal, S.S., McDowell, W.H., Wollheim, W.M., Johnson, T.A.N., Mayar, P.M., Belt, K.T., Pennino, M.J., 2015. Urban evolution: the role of water. Water 7, 4063–4087.
Klaus, J., McDonnell, J.J., 2013. Hydrograph separation using stable isotopes: review and evaluation. J. Hydrol. 505, 47–64.
Konrad, C.P., 2003. Effects of Urban Development on Floods. U.S. Geological Survey Fact Sheet FS-076–03, pp. 1–4.
Lee, J.G., Heaney, J.P., 2003. Estimation of urban imperviousness and its impacts on storm water systems. J. Water Resour. Plan. Manag. 129, 419–426.
Loperfido, J.V., Noe, G.B., Jarnagin, S.T., Hogan, D.M., 2014. Effects of distributed and centralized stormwater best management practices and land cover on urban stream hydrology at the catchment scale. J. Hydrol. 519, 2584–2595.
Lutzen, E.E., Rockaway Jr., J.D., 1989. Engineering Geologic Map of Saint Louis County, Missouri. Missouri Department of Natural Resources. Open File Mapp. 89–256-EG.
Marchi, L., Borga, M., Preciso, E., Gaume, E., 2010. Characterisation of selected extreme flash floods in Europe and implications for flood risk management. J. Hydrol. 394, 118–133.
Metropolitan Saint Louis Sewer District MSD, 2016. Metropolitan Saint Louis Sewer District, Metropolitan Saint Louis Sewer District Web page. http://www.stlmsd.com/home.
Meriano, M., Howard, K.W., Eyles, N., 2011. The role of midsummer urban aquifer recharge in stormflow generation using isotopic and chemical hydrograph separation techniques. J. Hydrol. 396, 82–93.
Missouri Department of Conservation MDC, 2005. LaBarque Creek Watershed: Conservation Opportunity Area, Missouri Department of Conservation Web page. http://mdc.mo.gov/.
Missouri Department of Natural Resources MoDNR, 2016. Missouri Water Quality: Missouri's 303(d) Streams and Lakes, Missouri Department of Natural Resources Web page. http://dnr.mo.gov/env/wpp/waterquality/303d/303d.htm.
Multi-Resolution Land Characteristics Consortium MRLC, 2016. National Land Cover Database 2006 (NLCD2006), NLCD2006 Web page. http://www.mrlc.gov/nlcd06_data.php.
Muñoz-Villers, L.E., McDonnell, J.J., 2012. Runoff generation in a steep, tropical montane cloud forest catchment on permeable volcanic substrate. Water Resour. Res. 48, W09528.
National Oceanic and Atmospheric Administration NOAA, 2016. National Weather Service (NWS) Weather, NWS Web page. http://www.weather.gov/.
O'Driscoll, M., Clinton, S., Jefferson, A., Manda, A., McMillan, S., 2010. Urbanization effects on watershed hydrology and in-stream processes in the southern United States. Water 2, 605–648.
Ogden, F.L., Sharif, H.O., Senarath, S.U.S., Smith, J.A., Baeck, M.L., Richardson, J.R., 2000. Hydrologic analysis of the Fort Collins, Colorado, flash flood of 1997. J. Hydrol. 228, 82–100.
Pellerin, B.A., Wollheim, W.M., Feng, X., Vörösmarty, C.J., 2008. The application of electrical conductivity as a tracer for hydrograph separation in urban catchments. Hydrol. Process. 22, 1810–1818.
Renshaw, C.E., Feng, X.H., Sinclair, K.J., Dums, R.H., 2003. The use of stream flow routing for direct channel precipitation with isotopically-based hydrograph separations: the role of new water in stormflow generation. J. Hydrol. 273, 205–216.
Shock, E.L., Carbery, K., Noblit, N., Schnall, B., Kogan, P., Rovito, S., Berg, A., Liang, J., 2003. Water and solute sources in an urban stream, River des Peres, Saint Louis, Missouri. In: Criss, R.E., Wilson, D.A. (Eds.), At the Confluence: Rivers, Floods, and Water Quality in the Saint Louis Region. Missouri Botanical Garden Press, Saint Louis, pp. 150–160.
Sklash, M.G., Farvolden, R.N., 1979. The role of groundwater in storm runoff. J. Hydrol. 43, 45–65.
Sklash, M.G., Stewart, M.K., Pearce, A.J., 1986. Storm runoff generation in humid headwater catchments: 2. A case study of hillslope and low-order stream response. Water Resour. Res. 22, 1273–1282.
Stueber, A.M., Criss, R.E., 2005. Origin and transport of dissolved chemicals in a karst watershed, southwestern Illinois. J. Am. Water Resour. Assoc. 41, 267–290.
U.S. Geological Survey USGS, 2016. USGS Current Water Data for Missouri. National Water Information System, Web Interface Web page. http://waterdata.usgs.gov/mo/nwis/rt.
Vicars-Groening, J., Williams, H.F.L., 2007. Impact of urbanization on storm response of White Rock Creek, Dallas, TX. Environ. Geol. 51, 1,263–1,269.
Walsh, C.J., Roy, A.H., Feminella, J.W., Cottingham, P.D., Groffman, P.M., Morgan II, R.P., 2005. The urban stream syndrome: current knowledge and the search for a cure. J. North Am. Benthol. Soc. 24, 706–723.
Winston, W.E., 2001. Dynamic Response of an Eastern Missouri Karst Spring to Seasonal and Storm Induced Perturbations [Masters thesis]. Washington University in Saint Louis, Saint Louis, p. 225.
Winston, W.E., Criss, R.E., 2004. Dynamic hydrologic and geochemical response in a perennial karst spring. Water Resour. Res. 40, W05106.